

# Damping Characteristics of Nonlocal Strain Gradient Waves in Thermoviscoelastic Graphene Sheets Subjected to Nonlinear Substrate Effects

R. Selvamani<sup>1\*</sup>, T. Prabhakaran<sup>1</sup>, and F. Ebrahimi<sup>2</sup>

<sup>1</sup>Department of Mathematics, Karunya Institute of Technology and Sciences, Coimbatore, Tamilnadu, 641114 India

<sup>2</sup>Department of Mechanical Engineering, Imam Khomieni International University, Qazvin, 34148-96818 Iran

\* e-mail: selvamani@karunya.edu

Received November 29, 2023; revised December 22, 2023; accepted December 26, 2023

**Abstract**—The present study explores dispersion characteristics of thermal, viscoelastic and mechanical waves in graphene sheets subjected to uniform thermal loading and supported by the visco-Pasternak foundation. Kinematic relations for graphene sheets are deduced within two-variable refined higher-order plate theory. Damping effects of the viscoelastic medium are modeled using the Kelvin–Voigt model. The research extensively investigates the size-dependent behavior of graphene sheets by incorporating nonlocal strain gradient theory. Nonlocal governing equations are formulated under Hamilton’s principle and solved analytically to determine wave frequency values. To validate the results, a comparative analysis is conducted, and the outcomes are tabulated to confirm the effectiveness of the approach. Finally, graphical representations are employed to depict the influence of each parameter on the wave propagation responses of graphene sheets.

**Keywords:** wave propagation, graphene sheets, nonlocal strain gradient theory, visco-Pasternak foundation, thermal loading

**DOI:** 10.1134/S1029959924040106

## 1. INTRODUCTION

In recent years, the enhanced quality properties of nanomaterials have caught the attention of numerous researchers. The significance of size effects becomes pronounced as structures reach very small dimensions, as evidenced by atomistic modeling and experimental studies. Consequently, the size effect plays a crucial role in shaping the mechanical behavior of micro- and nanostructures. There is a notable current trend within the scientific community towards exploring the mechanical behavior of structures using nanoscale elements. Given the substantial interest of a growing number of researchers in employing nanoscale beams and plates, it becomes imperative to acquire comprehensive knowledge about the size-dependent behavior of these diminutive elements. As a result, nonlocal continuum theories were developed to elucidate small-scale effects when investigating the mechanical characteristics of nanodevices. Eringen [1] proposed the first nonlocal theory, called nonlocal elasticity theory, which relates the stress state in a desired point not only to the strain of this

particular point but also to the strain of all adjacent points. This theory was employed by an abundant range of authors, and it is worth demonstrating some of the previous works gaining nonlocal elasticity during their study on the mechanical response of nanobeams or nanoplates. Evaluations of the contact problem of functionally graded materials via various analytical and numerical methods were exposed by Yaylacı et al. [2–14]. Wang et al. [15] analyzed the wave dispersion characteristics of nanoplates within nonlocal elasticity. The studies conducted by Ebrahimi et al. [16–19] are notable for the dynamic analysis of nanomaterials via size effects. Eltaher et al. [20] described the vibrational properties of nanobeams in the framework of the finite element method and Euler–Bernoulli beam theory. The bending vibration analysis of nanobeams was performed by Ghadiri and Shafiei [21] using the differential quadrature method. A few years later, researchers figured out that nonlocal elasticity theory was not powerful enough to completely estimate the behavior of small structures [22]. In other words, the stiffness-hardening be-

havior of nanostructures was neglected in nonlocal elasticity and only the stiffness-softening effect was included. This stimulated the development of a new nonlocal theory, called nonlocal strain gradient theory, to rectify the mentioned deficiency. Li and Hu [23] presented nonlocal strain gradient theory to highlight size effects while studying the buckling response of nanobeams. Examination of the thermomechanical buckling properties of orthotropic nanoplates was performed by Farajpour et al. [24] in the framework of nonlocal strain gradient theory. The constitutive equation of classical continuum mechanics does not consider size effects [25–34]. This makes it difficult to accurately describe thermal and mechanical engineering properties of nanomaterials. Continuum mechanics was used to address this issue as an alternative to small-scale investigations and molecular dynamics simulations. Narendar and Gopalakrishnan [35] dealt with surface effects on the wave propagation behavior of a nanoplate. Impact and reaction of thermal stresses on various functionally graded materials were discussed by Tounsi et al. [36–45] within different computational theories.

Graphene sheets possess some advantageous over other small structures made of different materials, such as higher elastic potential [46] and larger thermal conductivity [47]. According to the above information, it is necessary to obtain detailed results on the mechanical response of these types of nanostructures. Thus, Murmu and Pradhan [48] tried to show the dynamic response of embedded monolayer graphene sheets employing Eringen's nonlocal theory. Ansari and Rouhi [49] presented an atomistic finite element model for vibration and axial buckling analysis of monolayer graphene sheets. Size-dependent mechanical characteristics of propagating waves in graphene sheets were exactly studied by Arash et al. [50] within nonlocal elasticity. Furthermore, magnetomechanical vibration and stability analysis of monolayer graphene sheets rested on the viscoelastic foundation is the issue of another research performed by Ghorbanpour Arani et al. [51]. Xiao et al. [52] presented nonlocal strain gradient theory to examine the wave propagation behavior of viscoelastic monolayer graphene sheets.

The literature survey reveals that wave propagation characteristics of a graphene sheet on the viscoelastic medium under thermal loading has not yet been investigated. Henceforward, it is found necessary to survey this problem here for the first time. The graphene sheet is considered to rest on the visco-Pasternak substrate including a linear constant

(Winkler coefficient), a nonlinear constant (Pasternak coefficient) and a damping constant. Shear deformation is taken into account using a higher-order two-variable shear deformation plate theory. Moreover, nonlocal strain gradient theory is utilized to consider small-scale effects. Once the nonlocal differential equations are completely derived, they will be solved analytically using an exponential function. The influence of each parameter is precisely explained at the end of the paper.

## 2. THEORY AND FORMULATION

### 2.1. Kinematic Relations

The present section is devoted to the description of the kinematic behavior of graphene sheets. The schematic of an embedded monolayer graphene sheet can be seen in Fig. 1. In order to consider shear deformation effects, a refined higher-order plate theory is utilized. Thus, displacement fields can be written as [16]

$$U(x, y, z) = -z \frac{\partial w_b}{\partial x} - f(z) \frac{\partial w_s}{\partial x}, \quad (1)$$

$$V(x, y, z) = -z \frac{\partial w_b}{\partial y} - f(z) \frac{\partial w_s}{\partial y}, \quad (2)$$

$$W(x, y, z) = w_b(x, y) + w_s(x, y), \quad (3)$$

where  $w_b$  and  $w_s$  are the bending and shear deflections in the thickness direction, respectively, and  $f(z)$  is the shape function that estimates shear stress and shear strain. In the present theory, a trigonometric function is used as follows:

$$f(z) = z - \frac{h}{\pi} \sin\left(\frac{\pi z}{h}\right). \quad (4)$$

Here,  $h$  is the plate thickness, and, for shear stress and shear strain estimation, the shape functions are often associated with the deformation of the material within an element. Now, nonzero strains can be written as follows:

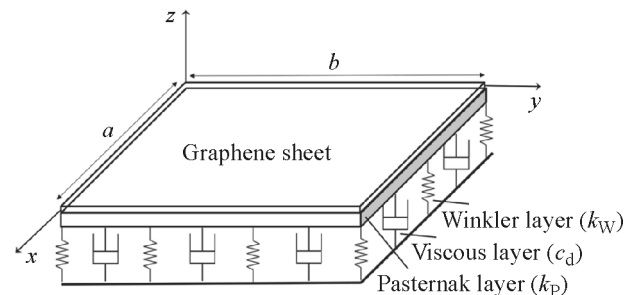


**Fig. 1.** Geometry of a monolayer graphene sheet rested on the viscoelastic medium.

$$\begin{Bmatrix} \varepsilon_x \\ \varepsilon_y \\ \gamma_{xy} \end{Bmatrix} = z \begin{Bmatrix} -\frac{\partial^2 w_b}{\partial x^2} \\ -\frac{\partial^2 w_b}{\partial y^2} \\ -2\frac{\partial^2 w_b}{\partial x \partial y} \end{Bmatrix} + f(z) \begin{Bmatrix} -\frac{\partial^2 w_s}{\partial x^2} \\ -\frac{\partial^2 w_s}{\partial y^2} \\ -2\frac{\partial^2 w_s}{\partial x \partial y} \end{Bmatrix}, \quad (5)$$

$$\begin{Bmatrix} \gamma_{yz} \\ \gamma_{xz} \end{Bmatrix} = g(z) \begin{Bmatrix} \frac{\partial w_s}{\partial y} \\ \frac{\partial w_s}{\partial x} \end{Bmatrix},$$

where  $g(z)$  can be stated as

$$g(z) = 1 - \frac{df(z)}{dz}. \quad (6)$$

Moreover, Hamilton's principle can be defined as

$$\int_0^t \delta(U - T + V) dt = 0, \quad (7)$$

in which  $U$  is the strain energy,  $T$  is the kinetic energy, and  $V$  is the work done by external loads. The variation of strain energy can be calculated as

$$\begin{aligned} \delta U = \int_V \sigma_{ij} \delta \varepsilon_{ij} dV = \int_V (\sigma_x \delta \varepsilon_x + \sigma_y \delta \varepsilon_y \\ + \sigma_{xy} \delta \gamma_{xy} + \sigma_{yz} \delta \gamma_{yz} + \sigma_{xz} \delta \gamma_{xz}) dV. \end{aligned} \quad (8)$$

Substituting Eq. (5) in Eq. (8) gives

$$\begin{aligned} \delta U = \int_0^a \int_0^b \left( -M_x^b \frac{\partial^2 \delta w_b}{\partial x^2} - M_x^s \frac{\partial^2 \delta w_s}{\partial x^2} - M_y^b \frac{\partial^2 \delta w_b}{\partial y^2} \right. \\ \left. - M_y^s \frac{\partial^2 \delta w_s}{\partial y^2} - 2M_{xy}^b \frac{\partial^2 \delta w_b}{\partial x \partial y} - 2M_{xy}^s \frac{\partial^2 \delta w_s}{\partial x \partial y} \right. \\ \left. + Q_{xz} \frac{\partial \delta w_s}{\partial x} + Q_{yz} \frac{\partial \delta w_s}{\partial y} \right) dy dx. \end{aligned} \quad (9)$$

In Eq. (9), the unknown parameters can be defined in the following form:

$$\begin{aligned} (M_i^b, M_i^s) &= \int_{-h/2}^{h/2} (z, f) \sigma_i dz, \quad i = (x, y, xy), \\ Q_i &= \int_{-h/2}^{h/2} g \sigma_i dz, \quad i = (xz, yz). \end{aligned} \quad (10)$$

Furthermore, the variation in work done by external forces can be shown as follows:

$$\begin{aligned} \delta V = \int_0^a \int_0^b \left( N_x^0 \frac{\partial(w_b + w_s)}{\partial x} \frac{\partial \delta(w_b + w_s)}{\partial x} \right. \\ \left. + N_y^0 \frac{\partial(w_b + w_s)}{\partial y} \frac{\partial \delta(w_b + w_s)}{\partial y} \right) \end{aligned}$$

$$\begin{aligned} + 2\delta N_{xy}^0 \frac{\partial(w_b + w_s)}{\partial x} \frac{\partial(w_b + w_s)}{\partial y} - k_W \delta(w_b + w_s) \\ - C_d \delta \frac{\partial(w_b + w_s)}{\partial t} + k_p \left( \frac{\partial(w_b + w_s)}{\partial x} \frac{\partial \delta(w_b + w_s)}{\partial x} \right. \\ \left. + \frac{\partial(w_b + w_s)}{\partial y} \frac{\partial \delta(w_b + w_s)}{\partial y} \right) dy dx, \end{aligned} \quad (11)$$

where  $N_x^0, N_y^0, N_{xy}^0$  are the in-plane applied loads,  $k_W$  is the Winkler coefficient,  $k_p$  is the Pasternak coefficient, and  $C_d$  is the damping coefficient. The variation in kinetic energy should be written as

$$\begin{aligned} \delta K = \int_0^a \int_0^b \left( I_0 \frac{\partial(w_b + w_s)}{\partial t} \frac{\partial \delta(w_b + w_s)}{\partial t} \right. \\ \left. + I_2 \left( \frac{\partial w_b}{\partial x} \frac{\partial \delta w_b}{\partial x} + \frac{\partial w_b}{\partial y} \frac{\partial \delta w_b}{\partial y} \right) \right. \\ \left. + K_2 \left( \frac{\partial w_s}{\partial x} \frac{\partial \delta w_s}{\partial x} + \frac{\partial w_s}{\partial y} \frac{\partial \delta w_s}{\partial y} \right) \right. \\ \left. + J_2 \left( \frac{\partial w_b}{\partial x} \frac{\partial \delta w_s}{\partial x} + \frac{\partial w_s}{\partial x} \frac{\partial \delta w_b}{\partial x} \right. \right. \\ \left. \left. + \frac{\partial w_b}{\partial y} \frac{\partial \delta w_s}{\partial y} + \frac{\partial w_s}{\partial y} \frac{\partial \delta w_b}{\partial y} \right) \right) dy dx, \end{aligned} \quad (12)$$

in which

$$(I_0, I_2, J_2, K_2) = \int_{-h/2}^{h/2} (1, z^2, zf, f^2) \rho dz. \quad (13)$$

By substituting Eqs. (9), (11), and (12) in Eq. (7) and setting the coefficients  $\delta w_b$  and  $\delta w_s$  to zero, the Euler-Lagrange equations of graphene sheets can be rewritten as

$$\begin{aligned} \frac{\partial^2 M_x^b}{\partial x^2} + 2 \frac{\partial^2 M_{xy}^b}{\partial x \partial y} + \frac{\partial^2 M_y^b}{\partial y^2} \\ + (k_p - N^T) \nabla^2 (w_b + w_s) - k_W (w_b + w_s) \\ - C_d \frac{\partial(w_b + w_s)}{\partial t} - I_0 \frac{\partial^2 (w_b + w_s)}{\partial t^2} \\ + I_2 \nabla^2 \left( \frac{\partial^2 w_b}{\partial t^2} \right) + J_2 \nabla^2 \left( \frac{\partial^2 w_s}{\partial t^2} \right) = 0, \end{aligned} \quad (14)$$

$$\begin{aligned} \frac{\partial^2 M_x^s}{\partial x^2} + 2 \frac{\partial^2 M_{xy}^s}{\partial x \partial y} + \frac{\partial^2 M_y^s}{\partial y^2} + \frac{\partial Q_{xz}}{\partial x} + \frac{\partial Q_{yz}}{\partial y} \\ + (k_p - N^T) \nabla^2 (w_b + w_s) - k_W (w_b + w_s) \\ - C_d \frac{\partial(w_b + w_s)}{\partial t} - I_0 \frac{\partial^2 (w_b + w_s)}{\partial t^2} \end{aligned}$$

$$+ J_2 \nabla^2 \left( \frac{\partial^2 w_b}{\partial t^2} \right) + K_2 \nabla^2 \left( \frac{\partial^2 w_s}{\partial t^2} \right) = 0, \quad (15)$$

where  $N_x^0 = N_y^0 = N^T$ ,  $N_{xy}^0 = 0$ , and thermal loading can be formulated as

$$N^T = \int_{-h/2}^{h/2} \frac{E}{1-\nu} \alpha \Delta T dz, \quad (16)$$

where  $E$ ,  $\nu$ ,  $\alpha$ , and  $\Delta T$  are Young's modulus, Poisson's ratio, thermal expansion coefficient, and temperature gradient, respectively.

### 2.2. Nonlocal Strain Gradient Elasticity

According to nonlocal strain gradient theory, the stress field takes into account the effects of the nonlocal elastic stress field, along with the strain gradient stress field. Therefore, for elastic solids, the theory can be expressed as follows [18]:

$$\sigma_{ij} = \sigma_{ij}^{(0)} - \frac{d\sigma_{ij}^{(1)}}{dx}. \quad (17)$$

Here, stresses  $\sigma_{xx}^{(0)}$  (classical stress) and  $\sigma_{xx}^{(1)}$  (higher-order stress) correspond to strain  $\epsilon_{xx}$  and strain gradient  $\epsilon_{xx,x}$ , respectively, as follows:

$$\begin{cases} \sigma_{ij}^{(0)} = \int_0^L C_{ijkl} \alpha_0(x, x', e_0 a) \epsilon'_{kl}(x') dx', \\ \sigma_{ij}^{(1)} = l^2 \int_0^L C_{ijkl} \alpha_1(x, x', e_1 a) \epsilon'_{kl,x}(x') dx', \end{cases} \quad (18)$$

where  $C_{ijkl}$  is the elastic coefficient,  $e_0 a$  and  $e_1 a$  are introduced to take account of nonlocal effects, and  $l$  takes account of strain gradient effects. Once the nonlocal kernel functions  $\alpha_0(x, x', e_0 a)$  and  $\alpha_1(x, x', e_1 a)$  satisfy the developed conditions, the constitutive relation of nonlocal strain gradient theory can be expressed as

$$\begin{aligned} (1 - (e_1 a)^2 \nabla^2)(1 - (e_0 a)^2 \nabla^2) \sigma_{ij} &= C_{ijkl} (1 - (e_1 a)^2 \nabla^2) \\ &\times \epsilon_{kl} - C_{ijkl} l^2 (1 - (e_0 a)^2 \nabla^2) \nabla^2 \epsilon_{kl}, \end{aligned} \quad (19)$$

where  $\nabla^2$  is the Laplacian operator. If  $e_1 = e_0 = e$ , the general constitutive relation in Eq. (19) becomes

$$(1 - (ea)^2 \nabla^2) \sigma_{ij} = C_{ijkl} (1 - l^2 \nabla^2) \epsilon_{kl}. \quad (20)$$

Finally, the simplified constitutive relation can be written as follows:

$$(1 - \mu^2 \nabla^2) \begin{Bmatrix} \sigma_x \\ \sigma_y \\ \sigma_{xy} \\ \sigma_{yz} \\ \sigma_{xz} \end{Bmatrix} = (1 - \eta^2 \nabla^2)$$

$$\times \begin{Bmatrix} Q_{11} & Q_{12} & 0 & 0 & 0 \\ Q_{12} & Q_{22} & 0 & 0 & 0 \\ 0 & 0 & Q_{66} & 0 & 0 \\ 0 & 0 & 0 & Q_{44} & 0 \\ 0 & 0 & 0 & 0 & Q_{55} \end{Bmatrix} \begin{Bmatrix} \epsilon_x \\ \epsilon_y \\ \gamma_{xy} \\ \gamma_{yz} \\ \gamma_{xz} \end{Bmatrix}. \quad (21)$$

In the above equation,

$$\begin{aligned} Q_{11} = Q_{22} &= \frac{E}{1-\nu^2}, \quad Q_{12} = \nu Q_{11}, \\ Q_{44} = Q_{55} = Q_{66} &= \frac{E}{2(1+\nu)}, \end{aligned} \quad (22)$$

where  $\mu = e_0 a$  and  $\eta = l$ . Substituting Eq. (10) in Eq. (21) and considering the Kelvin–Voigt viscoelastic model gives

$$\begin{aligned} (1 - \mu^2 \nabla^2) \begin{Bmatrix} M_x^b \\ M_y^b \\ M_{xy}^b \end{Bmatrix} &= \left( 1 + g \frac{\partial}{\partial t} \right) (1 - \eta^2 \nabla^2) \\ &\times \left( \begin{Bmatrix} D_{11} & D_{12} & 0 \\ D_{12} & D_{22} & 0 \\ 0 & 0 & D_{66} \end{Bmatrix} \begin{Bmatrix} -\frac{\partial^2 w_b}{\partial x^2} \\ -\frac{\partial^2 w_b}{\partial y^2} \\ -2\frac{\partial^2 w_b}{\partial x \partial y} \end{Bmatrix} \right. \\ &+ \left. \begin{Bmatrix} D_{11}^s & D_{12}^s & 0 \\ D_{12}^s & D_{22}^s & 0 \\ 0 & 0 & D_{66}^s \end{Bmatrix} \begin{Bmatrix} -\frac{\partial^2 w_s}{\partial x^2} \\ -\frac{\partial^2 w_s}{\partial y^2} \\ -2\frac{\partial^2 w_s}{\partial x \partial y} \end{Bmatrix} \right), \quad (23) \\ (1 - \mu^2 \nabla^2) \begin{Bmatrix} M_x^s \\ M_y^s \\ M_{xy}^s \end{Bmatrix} &= \left( 1 + g \frac{\partial}{\partial t} \right) (1 - \eta^2 \nabla^2) \\ &\times \left( \begin{Bmatrix} D_{11}^s & D_{12}^s & 0 \\ D_{12}^s & D_{22}^s & 0 \\ 0 & 0 & D_{66}^s \end{Bmatrix} \begin{Bmatrix} -\frac{\partial^2 w_b}{\partial x^2} \\ -\frac{\partial^2 w_b}{\partial y^2} \\ -2\frac{\partial^2 w_b}{\partial x \partial y} \end{Bmatrix} \right) \end{aligned}$$

$$+ \begin{pmatrix} H_{11}^s & H_{12}^s & 0 \\ H_{12}^s & H_{22}^s & 0 \\ 0 & 0 & H_{66}^s \end{pmatrix} \begin{Bmatrix} -\frac{\partial^2 w_s}{\partial x^2} \\ -\frac{\partial^2 w_s}{\partial y^2} \\ -2\frac{\partial^2 w_s}{\partial x \partial y} \end{Bmatrix}, \quad (24)$$

$$(1-\mu^2 \nabla^2) \begin{Bmatrix} Q_x \\ Q_y \end{Bmatrix} = \left(1 + g \frac{\partial}{\partial t}\right) (1-\eta^2 \nabla^2) \times \begin{pmatrix} A_{44}^s & 0 \\ 0 & A_{55}^s \end{pmatrix} \begin{Bmatrix} \frac{\partial w_s}{\partial x} \\ \frac{\partial w_s}{\partial y} \end{Bmatrix}. \quad (25)$$

In Eqs. (23) to (25), the cross-sectional rigidities can be formulated as follows:

$$\begin{pmatrix} D_{11} & D_{11}^s & H_{11}^s \\ D_{12} & D_{12}^s & H_{12}^s \\ D_{66} & D_{66}^s & H_{66}^s \end{pmatrix} = \int_{-h/2}^{h/2} Q_{11} \begin{pmatrix} z^2 & zf & f^2 \end{pmatrix} \begin{Bmatrix} 1 \\ \nu \\ \frac{1-\nu}{2} \end{Bmatrix} dz, \quad (26)$$

$$A_{44}^s = A_{55}^s = \int_{-h/2}^{h/2} g^2 \frac{E}{2(1+\nu)} dz. \quad (27)$$

By substituting Eqs. (23) to (25) in Eqs. (14) and (15), the nonlocal governing equations of monolayer graphene sheets can be directly derived in terms of displacements as follows:

$$\begin{aligned} & \left(1 + g \frac{\partial}{\partial t}\right) (1-\eta^2 \nabla^2) \\ & \times \left( -D_{11} \frac{\partial^4 w_b}{\partial x^4} - 2(D_{12} + 2D_{66}) \frac{\partial^4 w_b}{\partial x^2 \partial y^2} - D_{22} \frac{\partial^4 w_b}{\partial y^4} \right. \\ & \left. - D_{11}^s \frac{\partial^4 w_s}{\partial x^4} - 2(D_{12}^s + 2D_{66}^s) \frac{\partial^4 w_s}{\partial x^2 \partial y^2} - D_{22}^s \frac{\partial^4 w_s}{\partial y^4} \right) \\ & + (1-\mu^2 \nabla^2) \left( -I_0 \frac{\partial^2 (w_b + w_s)}{\partial t^2} \right. \\ & \left. + I_2 \left( \frac{\partial^4 w_b}{\partial x^2 \partial t^2} + \frac{\partial^4 w_b}{\partial y^2 \partial t^2} \right) + J_2 \left( \frac{\partial^4 w_s}{\partial x^2 \partial t^2} + \frac{\partial^4 w_s}{\partial y^2 \partial t^2} \right) \right) \end{aligned}$$

$$+ (k_p - N^T) \left( \frac{\partial^2 (w_b + w_s)}{\partial x^2} + \frac{\partial^2 (w_b + w_s)}{\partial y^2} \right) - \left( k_w + \frac{\partial}{\partial t} C_d \right) (w_b + w_s) = 0, \quad (28)$$

$$\begin{aligned} & \left(1 + g \frac{\partial}{\partial t}\right) (1-\eta^2 \nabla^2) \left( -D_{11}^s \frac{\partial^4 w_b}{\partial x^4} \right. \\ & \left. - 2(D_{12}^s + 2D_{66}^s) \frac{\partial^4 w_b}{\partial x^2 \partial y^2} - D_{22}^s \frac{\partial^4 w_b}{\partial y^4} \right. \\ & \left. - H_{11}^s \frac{\partial^4 w_s}{\partial x^4} - 2(H_{12}^s + 2H_{66}^s) \frac{\partial^4 w_s}{\partial x^2 \partial y^2} \right. \\ & \left. - H_{22}^s \frac{\partial^4 w_s}{\partial y^4} + A_{44}^s \frac{\partial^2 w_s}{\partial x^2} + A_{55}^s \frac{\partial^2 w_s}{\partial y^2} \right) \\ & + (1-\mu^2 \nabla^2) \left( -I_0 \frac{\partial^2 (w_b + w_s)}{\partial t^2} + J_2 \right. \\ & \left. \times \left( \frac{\partial^4 w_b}{\partial x^2 \partial t^2} + \frac{\partial^4 w_b}{\partial y^2 \partial t^2} \right) + K_2 \left( \frac{\partial^4 w_s}{\partial x^2 \partial t^2} + \frac{\partial^4 w_s}{\partial y^2 \partial t^2} \right) \right. \\ & \left. + (k_p - N^T) \left( \frac{\partial^2 (w_b + w_s)}{\partial x^2} + \frac{\partial^2 (w_b + w_s)}{\partial y^2} \right) \right. \\ & \left. - \left( k_w + \frac{\partial}{\partial t} C_d \right) (w_b + w_s) \right) = 0. \quad (29) \end{aligned}$$

### 3. SOLUTION PROCEDURE

In this section, the derived nonlocal governing equations will be solved analytically. The displacement fields are assumed to be exponential and can be defined as follows:

$$\begin{cases} w_b(x, y, t) \\ w_s(x, y, t) \end{cases} = \begin{cases} W_b \exp[i(\beta_1 x + \beta_2 y - \omega t)] \\ W_s \exp[i(\beta_1 x + \beta_2 y - \omega t)] \end{cases}, \quad (30)$$

where  $W_b$  and  $W_s$  are the unknown coefficients,  $\beta_1$  and  $\beta_2$  are the wave numbers of wave propagation along the  $x$  and  $y$  directions, respectively, and  $\omega$  is the angular frequency of a wave. Substituting Eq. (30) in Eqs. (28) and (29) yields

$$([K]_{2 \times 2} - \omega^2 [M]_{2 \times 2}) \{\Delta\} = \{0\}, \quad (31)$$

where the corresponding  $k_{ij}$  and  $m_{ij}$  are defined in Appendix A. The unknown parameters of Eq. (31) can be noted as follows:

$$\{\Delta\} = \{W_b, W_s\}^T. \quad (32)$$

In order to derive the angular frequency, the determinant of the left-hand side of Eq. (32) should be set to zero:

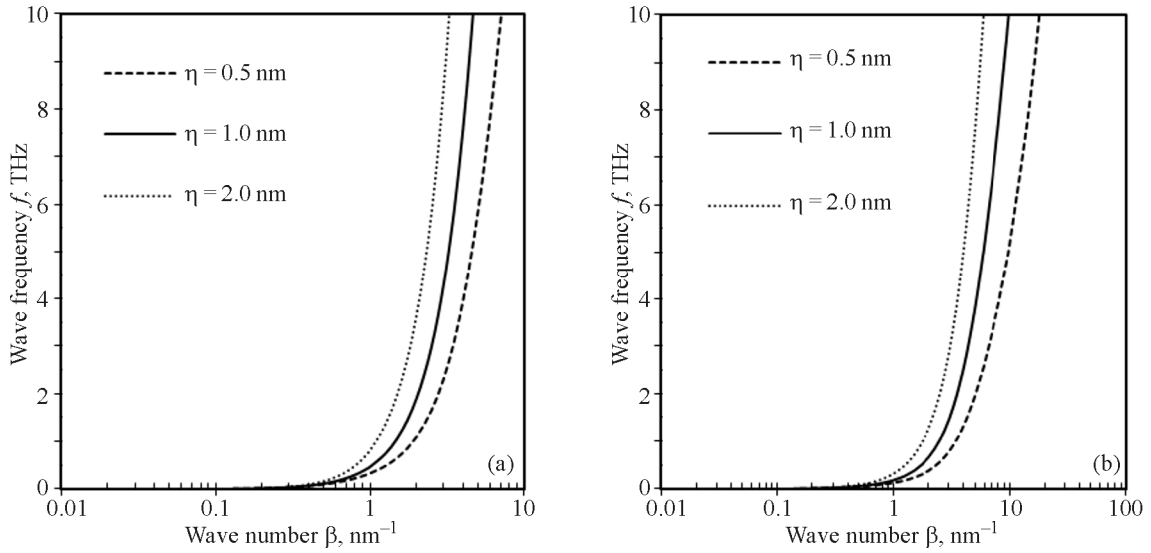


**Fig. 2.** Wave frequency versus wave number for various length scale parameters at  $\mu = 1$  (a) and  $3 \text{ nm}$  (b).  $k_w = k_p = 0$ ,  $C_d = 0$ ,  $g = 0$ , and  $\Delta T = 0$ .

$$\left| [K]_{2 \times 2} - \omega^2 [M]_{2 \times 2} \right| = 0. \quad (33)$$

In the above equation, by setting  $\beta_1 = \beta_2 = \beta$  and solving the obtained equation for  $\omega$ , the angular frequency of a wave in the embedded monolayer graphene sheet can be calculated.

#### 4. RESULTS AND DISCUSSION

Here, the wave propagation responses of monolayer graphene sheets are supposed to be changed depending on various parameters. The thermomechanical properties of graphene sheets are  $E = 1 \text{ TPa}$ ,  $\nu = 0.19$ ,  $\rho = 2300 \text{ kg/m}^3$ , and  $\alpha = 1.6 \times 10^{-6} \text{ 1/K}$ . The thickness is presumed to be  $h = 0.34 \text{ nm}$ . In the diagrams, wave frequencies are calculated by dividing the angular frequency of a wave by  $2\pi$  ( $f = \omega/(2\pi)$ ). Figure 2 is plotted to describe the small-scale effects while changing the wave frequency. It is seen that at a lower nonlocal parameter the slope of the curve is steeper, which means that at the constant wave number the wave frequency grows easier when the nonlocal parameter is smaller. Indeed, this phenomenon suggests a softening impact which is attributed to the nonlocal parameter introduced by Eringen. Conversely, the length scale parameter operates in a manner that increases the wave frequency. To put it differently, elevating the length scale parameter evidently leads to higher wave frequencies. In essence, the length scale parameter accommodates the stiffness-hardening effect observed in nanoscale structures,

which is not taken into account by the nonlocal parameter.

The damping effect becomes more powerful with increasing structural damping coefficient. Even though the curve shape is similar for all nonzero structural damping coefficients, the wave number at which the wave frequency is maximum is not equal for various values of this coefficient. In other words, the peak of the curve moves to the left as the structural damping coefficient increases. On the other hand, Fig. 3 is plotted to magnify the combined influence of the small size and damping coefficient. From the given figures it is obvious that there are two size-dependent ways for increasing the wave frequency of graphene sheets. The first approach is to use smaller nonlocal parameters, and the second one is to choose higher values for the length scale parameter. Judging from the diagrams, the wave frequency shows a damping behavior. As a matter of fact, the wave frequency can be smaller whatever the damping coefficient value is. It should be also noted that, at the final damping coefficient which is about 12 in this case, the wave frequency reaches a unit value which is exactly zero. Now, we turn to the investigation of the effect of the Winkler and Pasternak coefficients by plotting the wave frequency versus damping coefficients in Fig. 4. It is clearly seen that both the Winkler (linear) and Pasternak (nonlinear) coefficients have enough potential to amplify wave frequency values. Moreover, the strongest change in the wave frequency response can be observed when the Winkler

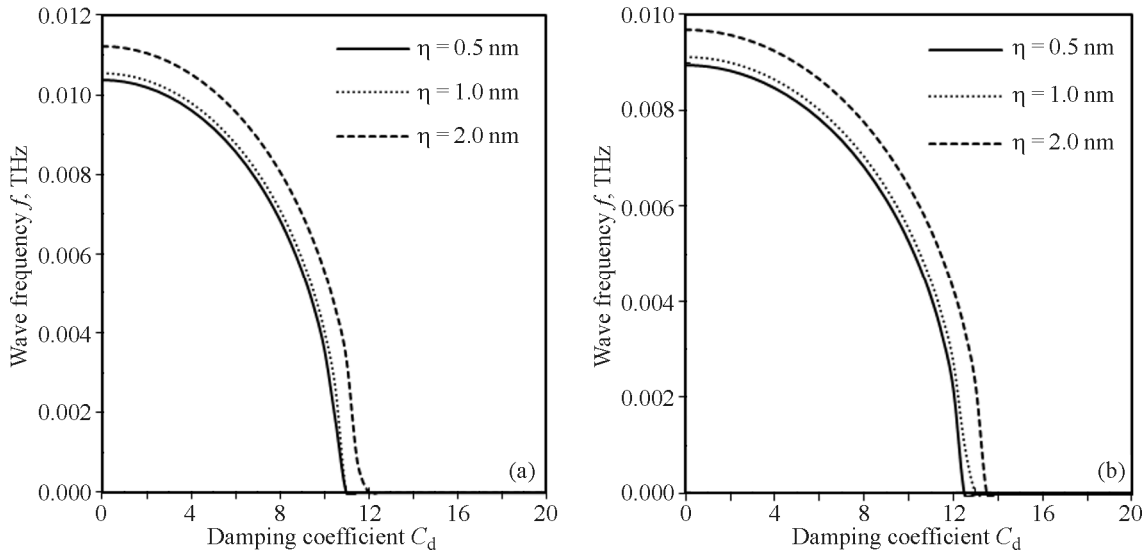


**Fig. 3.** Wave frequency versus damping coefficient for different length scale parameters at  $\mu = 1$  (a) and 3 nm (b).  $k_W = k_P = 0$ ,  $\Delta T = 0$ ,  $q = 0$ , and  $\beta = 0.15 \times 10^9$  m.

coefficient varies from  $k_W = 0$  to  $k_W = 2.5$ . In other words, the initial shift in the Winkler or Pasternak coefficient from zero to their first nonzero value has the most significant impact on the wave frequency. Next we analyze the variation in the wave frequency by plotting the wave frequency against the Pasternak and Winkler coefficients at various temperature gradients in Fig. 5. It becomes apparent that higher temperature gradients result in lower wave frequencies. Furthermore, comparison shows that the Winkler

foundation model yields higher wave frequency values.

### 5. CONCLUSIONS

The present work was devoted to the investigation of the thermally affected wave propagation behavior of monolayer isotropic graphene sheets embedded on the viscoelastic substrate. The small-scale effects were estimated by using nonlocal strain gradient theory. Final governing equations were derived within

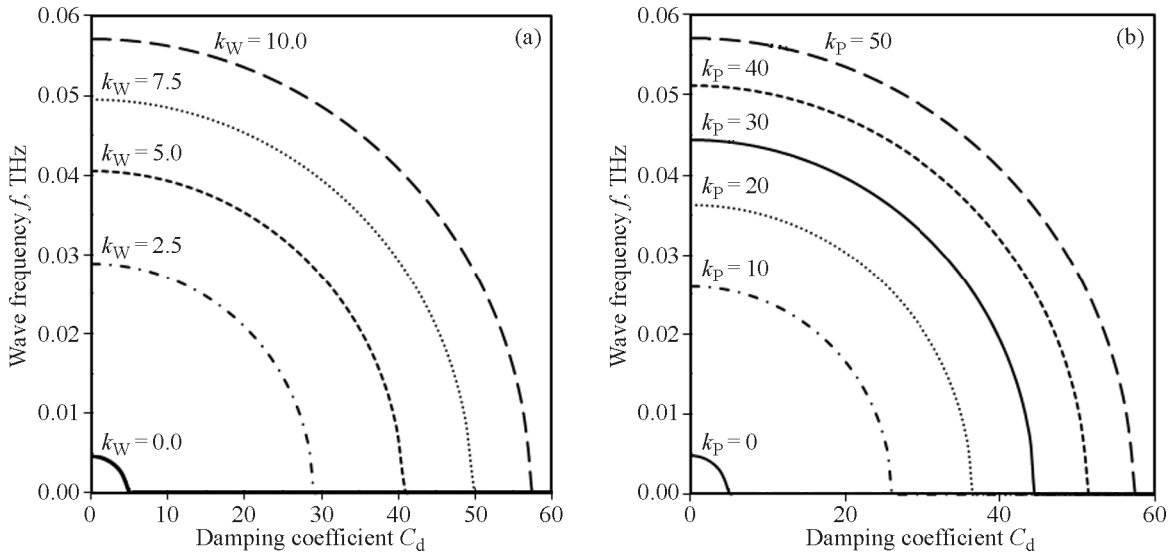


**Fig. 4.** Wave frequency versus damping coefficient for different Winkler ( $k_P = 0$ ) (a) and Pasternak coefficients ( $k_W = 0$ ) (b).  $\mu = \eta = 1$  nm,  $g = 1$ ,  $\Delta T = 0$ , and  $\beta = 0.1 \times 10^9$  m.

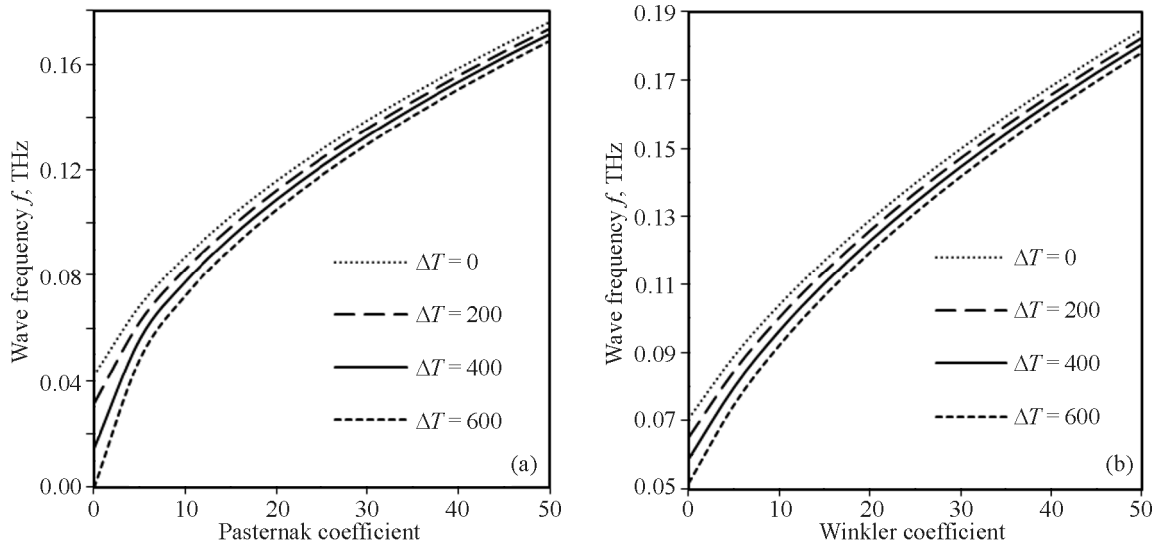


**Fig. 5.** Wave frequency versus Pasternak (a) and Winkler coefficients (b) for different temperature gradients.  $\mu = \eta = 1 \text{ nm}$ ,  $C_d = 0$ ,  $g = 1$ , and  $\beta = 0.3 \times 10^9 \text{ m}$ .

the Hamiltonian approach, and the obtained eigenvalue equation was solved by means of an exponential function to determine wave frequency values. The performed calculations reveal that

- (i) adding the length scale parameter increases wave frequency;
- (ii) reducing the nonlocal parameter may result in the wave frequency increase;
- (iii) amplifying the temperature gradient reduces wave frequency values.

These results may be useful in the design of thermoviscoelastic structural components of nanoelectromechanical systems (NEMS) operating in different environments, and the derived numerical results may serve as benchmarks for future damping analysis of structures containing graphene sheets.

#### APPENDIX A

In Eq. (31),  $k_{ij}$  and  $m_{ij}$  ( $i, j = 1, 2$ ) are defined as follows:

$$\begin{aligned}
 k_{11} = & -\left(1 + g \frac{\partial}{\partial t}\right) (1 + \eta^2 (\beta_1^2 + \beta_2^2)) (D_{11} \beta_1^4 \\
 & + 2(D_{12} + 2D_{66}) \beta_1^2 \beta_2^2 + D_{22} \beta_2^4) + (1 + \mu^2 \\
 & \times (\beta_1^2 + \beta_2^2)) ((N^T - k_p) (\beta_1^2 + \beta_2^2) - k_w - i\omega C_d), \\
 k_{12} = & -\left(1 + g \frac{\partial}{\partial t}\right) (1 + \eta^2 (\beta_1^2 + \beta_2^2)) (D_{11}^s \beta_1^4 \\
 & + 2(D_{12}^s + 2D_{66}^s) \beta_1^2 \beta_2^2 + D_{22}^s \beta_2^4) + (1 + \mu^2 \\
 & \times (\beta_1^2 + \beta_2^2)) ((N^T - k_p) (\beta_1^2 + \beta_2^2) - k_w - i\omega C_d), \quad (A1)
 \end{aligned}$$

$$\begin{aligned}
 k_{21} = & -\left(1 + g \frac{\partial}{\partial t}\right) (1 + \eta^2 (\beta_1^2 + \beta_2^2)) \\
 & \times (D_{11}^s \beta_1^4 + 2(D_{12}^s + 2D_{66}^s) \beta_1^2 \beta_2^2 + D_{22}^s \beta_2^4) \\
 & + (1 + \mu^2 (\beta_1^2 + \beta_2^2)) ((N^T - k_p) \\
 & \times (\beta_1^2 + \beta_2^2) - k_w - i\omega C_d), \\
 k_{22} = & -\left(1 + g \frac{\partial}{\partial t}\right) (1 + \eta^2 (\beta_1^2 + \beta_2^2)) \\
 & \times (H_{11}^s \beta_1^4 + 2(H_{12}^s + 2H_{66}^s) \beta_1^2 \beta_2^2 + H_{22}^s \beta_2^4 \\
 & + A_{55}^s \beta_1^2 + A_{44}^s \beta_2^2) + (1 + \mu^2 (\beta_1^2 + \beta_2^2)) \\
 & \times ((N^T - k_p) (\beta_1^2 + \beta_2^2) - k_w - i\omega C_d), \\
 m_{11} = & -(1 + \mu^2 (\beta_1^2 + \beta_2^2)) (I_0 + I_2 (\beta_1^2 + \beta_2^2)), \\
 & m_{12} = m_{21} \\
 & = -(1 + \mu^2 (\beta_1^2 + \beta_2^2)) (I_0 + J_2 (\beta_1^2 + \beta_2^2)), \quad (A2) \\
 m_{22} = & -(1 + \mu^2 (\beta_1^2 + \beta_2^2)) (I_0 + K_2 (\beta_1^2 + \beta_2^2)).
 \end{aligned}$$

#### FUNDING

This work was supported by ongoing institutional funding. No additional grants to carry out or direct this particular research were obtained.

#### CONFLICT OF INTEREST

The authors of this work declare that they have no conflicts of interest.



## REFERENCES

1. Eringen, A.C., Linear Theory of Nonlocal Elasticity and Dispersion of Plane Waves, *Int. J. Eng. Sci.*, 1972, vol. 10(5), pp. 425–435. [https://doi.org/10.1016/0020-7225\(72\)90050-X](https://doi.org/10.1016/0020-7225(72)90050-X)
2. Yaylacı, M., Şabano, B.Ş., Özdemir, M.E., and Birinci, A., Solving the Contact Problem of Functionally Graded Layers Resting on a HP and Pressed with a Uniformly Distributed Load by Analytical and Numerical Methods, *Struct. Eng. Mech.*, 2022, vol. 82(3), pp. 401–416. <https://doi.org/10.12989/sem.2022.82.3.401>
3. Turan, M., Uzun Yaylacı, E., and Yaylacı, M., Free Vibration and Buckling of Functionally Graded Porous Beams Using Analytical, Finite Element, and Artificial Neural Network Methods, *Arch. Appl. Mech.*, 2023, vol. 93(4), pp. 1351–1372. <https://doi.org/10.1007/s00419-022-02332-w>
4. Yaylacı, E.U., Öner, E., Yaylacı, M., Özdemir, M.E., Abushattal, A., and Birinci, A., Application of Artificial Neural Networks in the Analysis of the Continuous Contact Problem, *Struct. Eng. Mech.*, 2022, vol. 84(1), pp. 35–48. <https://doi.org/10.12989/sem.2022.84.1.035>
5. Yaylacı, M., Abanoz, M., Yaylacı, E.U., Ölmez, H., Sekban, D.M., and Birinci, A., Evaluation of the Contact Problem of Functionally Graded Layer Resting on Rigid Foundation Pressed Via Rigid Punch by Analytical and Numerical (FEM and MLP) Methods, *Arch. Appl. Mech.*, 2022, vol. 92(6), pp. 1953–1971. <https://doi.org/10.1007/s00419-022-02159-5>
6. Yaylacı, M., Yaylacı, E.U., Özdemir, M.E., Öztürk, Ş., and Sesli, H., Vibration and Buckling Analyses of FGM Beam with Edge Crack: Finite Element and Multilayer Perceptron Methods, *Steel Compos. Struct.*, 2023, vol. 46(4), pp. 565–575. <https://doi.org/10.12989/scs.2023.46.4.565>
7. Özdemir, M.E. and Yaylacı, M., Research of the Impact of Material and Flow Properties on Fluid–Structure Interaction in Cage Systems, *Wind Struct. Int. J.*, 2023, vol. 36(1), p. 31. <https://doi.org/10.12989/was.2023.36.1.031>
8. Adiyaman, G., Öner, E., Yaylacı, M., and Birinci, A., A Study on the Contact Problem of a Layer Consisting of Functionally Graded Material (FGM) in the Presence of Body Force, *J. Mech. Mater. Struct.*, 2023, vol. 18(1), pp. 125–141. <https://doi.org/10.2140/jomms.2023.18.125>
9. Yaylacı, M., Simulate of Edge and an Internal Crack Problem and Estimation of Stress Intensity Factor through Finite Element Method, *Adv. Nano Res.*, 2022, vol. 12(4), p. 405. <https://doi.org/10.12989/anr.2022.12.4.405>
10. Yaylacı, M., Uzun Yaylacı, E., Özdemir, M.E., Ay, S., and Öztürk, S., Implementation of Finite Element and Artificial Neural Network Methods to Analyze the Contact Problem of a Functionally Graded Layer Containing Crack, *Steel Compos. Struct.*, 2022, vol. 45(4), pp. 501–511. <https://doi.org/10.12989/scs.2022.45.4.501>
11. Yaylacı, M., The Investigation Crack Problem through Numerical Analysis, *Struct. Eng. Mech.*, 2016, vol. 57(6), pp. 1143–1156. <https://doi.org/10.12989/sem.2016.57.6.1143>
12. Yaylacı, M., Abanoz, M., Yaylacı, E.U., Ölmez, H., Sekban, D.M., and Birinci, A., The Contact Problem of the Functionally Graded Layer Resting on Rigid Foundation Pressed Via Rigid Punch, *Steel Compos. Struct.*, 2022, vol. 43(5), p. 661. <https://doi.org/10.12989/scs.2022.43.5.661>
13. Öner, E., Şengül Şabano, B., Uzun Yaylacı, E., Adiyaman, G., Yaylacı, M., and Birinci, A., On the Plane Receding Contact between Two Functionally Graded Layers Using Computational, Finite Element and Artificial Neural Network Methods, *Z. Angew. Math. Mech.*, 2022, vol. 102(2), p. e202100287. <https://doi.org/10.1002/zamm.202100287>
14. Yaylacı, M., Yayli, M., Yaylacı, E.U., Ölmez, H., and Birinci, A., Analyzing the Contact Problem of a Functionally Graded Layer Resting on an Elastic Half Plane with Theory of Elasticity, Finite Element Method and Multilayer Perceptron, *Struct. Eng. Mech.*, 2021, vol. 78(5), pp. 585–597. <https://doi.org/10.12989/sem.2021.78.5.585>
15. Wang, Y.Z., Li, F.M., and Kishimoto, K., Scale Effects on the Longitudinal Wave Propagation in Nanoplates, *Phys. E. Low-Dimens. Syst. Nanostructures*, 2010, vol. 42(5), pp. 1356–1360. <https://doi.org/10.1016/j.physe.2009.11.036>
16. Ebrahimi, F., Jafari, A., and Selvamani, R., Thermal Buckling Analysis of Magneto Electro Elastic Porous FG Beam in Thermal Environment, *Adv. Nano Res.*, 2020, vol. 8(1), pp. 83–94. <https://doi.org/10.12989/anr.2020.8.1.083>
17. Ebrahimi, F., Karimiasl, M., and Selvamani, R., Bending Analysis of Magneto-Electro Piezoelectric Nanobeams System under Hygro-Thermal Loading, *Adv. Nano Res.*, 2020, vol. 8(3), pp. 203–214. <https://doi.org/10.12989/anr.2020.8.3.203>
18. Ebrahimi, F., Kokaba, M., Shaghghi, G., and Selvamani, R., Dynamic Characteristics of Hygro-Magneto-Thermo-Electrical Nanobeam with Non-Ideal Boundary Conditions, *Adv. Nano Res.*, 2020, vol. 8(2), pp. 169–182. <https://doi.org/10.12989/anr.2020.8.2.169>
19. Ebrahimi, F., Hamed Hosseini, S., and Selvamani, R., Thermo-Electro-Elastic Nonlinear Stability Analysis of Viscoelastic Double-Piezonanoplates under Magnetic Field, *Struct. Eng. Mech.*, 2020, vol. 73(5), pp. 565–584.
20. Eltaher, M.A., Alshorbagy, A.E., and Mahmoud, F.F., Vibration Analysis of Euler–Bernoulli Nanobeams by Using Finite Element Method, *Appl. Math. Model.*, 2013, vol. 37(7), pp. 4787–4797. <https://doi.org/10.1016/j.apm.2012.10.016>

21. Ghadiri, M. and Shafiei, N., Nonlinear Bending Vibration of a Rotating Nanobeam Based on Nonlocal Eringen's Theory Using Differential Quadrature Method, *Microsyst. Technol.*, 2016, vol. 22(12), pp. 2853–2867. <https://doi.org/10.1007/s00542-015-2662-9>
22. Lam, D.C.C., Yang, F., and Chong, A.C.M., Experiments and Theory in Strain Gradient Elasticity, *J. Mech. Phys. Solids*, 2003, vol. 51(8), pp. 1477–1508. [https://doi.org/10.1016/S0022-5096\(03\)00053-X](https://doi.org/10.1016/S0022-5096(03)00053-X)
23. Li, L. and Hu, Y., Buckling Analysis of Size-Dependent Nonlinear Beams Based on a Nonlocal Strain Gradient Theory, *Int. J. Eng. Sci.*, 2015, vol. 97, pp. 84–94. <https://doi.org/10.1016/j.ijengsci.2015.08.013>
24. Farajpour, A., Yazdi, M.R.H., and Rastgoo, A.A., Higher-Order Nonlocal Strain Gradient Plate Model for Buckling of Orthotropic Nanoplates in Thermal Environment, *Acta Mech.*, 2016, vol. 227(7), pp. 1849–1867. <https://doi.org/10.1007/s00707-016-1605-6>
25. Selvamani, R. and Ponnusamy, P., Damping of Generalized Thermoelastic Waves in a Homogeneous Isotropic Plate, *Mater. Phys. Mech.*, 2012, vol. 14(1), pp. 64–73.
26. Selvamani, R., Influence of Thermo-Piezoelectric Field in a Circular Bar Subjected to Thermal Loading due to Laser Pulse, *Mater. Phys. Mech.*, 2016, vol. 27(1), pp. 1–8.
27. Selvamani, R., Free Vibration Analysis of Rotating Piezoelectric Bar of Circular Cross Section Immersed in Fluid, *Mater. Phys. Mech.*, 2015, vol. 24(1), pp. 24–34.
28. Selvamani, R., Dynamic Response of a Heat Conducting Solid Bar of Polygonal Cross Sections Subjected to Moving Heat Source, *Mater. Phys. Mech.*, 2014, vol. 21(2), pp. 177–193.
29. Selvamani, R. and Ponnusamy, P., Elasto Dynamic Wave Propagation in a Transversely Isotropic Piezoelectric Circular Plate Immersed in Fluid, *Mater. Phys. Mech.*, 2013, vol. 17(2), pp. 164–177.
30. Selvamani, R. and Ponnusamy, P., Effect of Rotation in an Axisymmetric Vibration of a Transversely Isotropic Solid Bar Immersed in an Inviscid Fluid, *Mater. Phys. Mech.*, 2012, vol. 15(2), pp. 97–106.
31. Selvamani, R. and Sujitha, G., Effect of Non-Homogeneity in a Magneto Electro Elastic Plate of Polygonal Cross-Sections, *Mater. Phys. Mech.*, 2018, vol. 40(1), pp. 84–103.
32. Selvamani, R., Flexural Wave Motion in a Heat Conducting Doubly Connected Thermo-Elastic Plate of Polygonal Cross-Sections, *Mater. Phys. Mech.*, 2014, vol. 19(1), pp. 51–67.
33. Selvamani, R. and Ponnusamy, P., Generalized Thermoelastic Waves in a Rotating Ring Shaped Circular Plate Immersed in an Inviscid Fluid, *Mater. Phys. Mech.*, 2013, vol. 18(1), pp. 77–92.
34. Selvamani, R. and Ponnusamy, P., Extensional Waves in a Transversely Isotropic Solid Bar Immersed in an Inviscid Fluid Calculated Using Chebyshev Polynomials, *Mater. Phys. Mech.*, 2013, vol. 16(1), pp. 82–91.
35. Narendar, S. and Gopalakrishnan, S., Study of Terahertz Wave Propagation Properties in Nanoplates with Surface and Small-Scale Effects, *Int. J. Mech. Sci.*, 2012, vol. 64(1), pp. 221–231. <https://doi.org/10.1016/j.ijmecsci.2012.06.012>
36. Bounouara, F., Sadoun, M., Saleh, M.M.S., Chikh, A., Bousahla, A.A., Kaci, A., and Tounsi, A., Effect of Visco-Pasternak Foundation on Thermo-Mechanical Bending Response of Anisotropic Thick Laminated Composite Plates, *Steel Compos. Struct.*, 2023, vol. 47(6), p. 693707. <https://doi.org/10.12989/SCS.2023.47.6.693>
37. Khorasani, M., Lampani, L., and Tounsi, A., A Refined Vibrational Analysis of the FGM Porous Type Beams Resting on the Silica Aerogel Substrate, *Steel Compos. Struct.*, 2023, vol. 47(5), pp. 633–644.
38. Tounsi, A., Bousahla, A.A., Tahir, S.I., Mostefa, A.H., Bourada, F., Al-Osta, M.A., and Tounsi, A., Influences of Different Boundary Conditions and Hygro-Thermal Environment on the Free Vibration Responses of FGM Sandwich Plates Resting on Viscoelastic Foundation, *Int. J. Struct. Stab.*, 2023, p. 2450117. <https://doi.org/10.1142/S0219455424501190>
39. Tounsi, A., Mostefa, A.H., Attia, A., Bousahla, A.A., Bourada, F., Tounsi, A., and Al-Osta, M.A., Free Vibration Investigation of Functionally Graded Plates with Temperature Dependent Properties Resting on a Viscoelastic Foundation, *Struct. Eng. Mech.*, 2023, vol. 86(1), p. 1. <https://doi.org/10.12989/sem.2023.86.1.001>
40. Tounsi, A., Mostefa, A.H., Bousahla, A.A., Tounsi, A., Ghazwani, M.H., Bourada, F., and Bouhadra, A., Thermodynamical Bending Analysis of P-FG Sandwich Plates Resting on Nonlinear Visco-Pasternak's Elastic Foundations, *Steel Compos. Struct.*, 2023, vol. 49(3), pp. 307–323. <https://doi.org/10.12989/scs.2023.49.3.307>
41. Belbachir, N., Bourada, F., Bousahla, A.A., Tounsi, A., Al-Osta, M.A., Ghazwani, M.H., and Tounsi, A.A., Refined Quasi-3D Theory for Stability and Dynamic Investigation of Cross-Ply Laminated Composite Plates on Winkler–Pasternak Foundation, *Struct. Eng. Mech.*, 2023, vol. 85(4), p. 433. <https://doi.org/10.12989/sem.2023.85.4.433>
42. Mudhaffar, I.M., Chikh, A., Tounsi, A., Al-Osta, M.A., Al-Zahrani, M.M., and Al-Dulaijan, S.U., Impact of Viscoelastic Foundation on Bending Behavior of FG Plate Subjected to Hygro-Thermo-Mechanical Loads, *Struct. Eng. Mech.*, 2023, vol. 86(2), p. 167. <https://doi.org/10.12989/sem.2023.86.2.167>
43. Zaitoun, M.W., Chikh, A., Tounsi, A., Sharif, A., Al-Osta, M.A., Al-Dulaijan, S.U., and Al-Zahrani, M.M., An Efficient Computational Model for Vibration Behavior of a Functionally Graded Sandwich Plate in a

- Hygrothermal Environment with Viscoelastic Foundation Effects, *Eng. Comput.*, 2023, vol. 39(2), pp. 1127–1141. <https://doi.org/10.1007/s00366-021-01498-1>
44. Tahir, S.I., Tounsi, A., Chikh, A., Al-Osta, M.A., Al-Dulajjan, S.U., and Al-Zahrani, M.M., The Effect of Three-Variable Viscoelastic Foundation on the Wave Propagation in Functionally Graded Sandwich Plates Via a Simple Quasi-3D HSDT, *Steel Compos. Struct.*, 2022, vol. 42(4), p. 501. <https://doi.org/10.12989/scs.2022.42.4.501>
45. Bouafia, K., Selim, M.M., Bourada, F., Bousahla, A.A., Bourada, M., Tounsi, A., and Tounsi, A., Bending and Free Vibration Characteristics of Various Compositions of FG Plates on Elastic Foundation Via Quasi 3D HSDT Model, *Steel Compos. Struct.*, 2021, vol. 41(4), pp. 487–503.
46. Lee, C., Wei, X., and Kysar, J.W., Measurement of the Elastic Properties and Intrinsic Strength of Monolayer Graphene, *Science*, 2008, vol. 321(5887), pp. 385–388. <https://doi.org/10.1126/science.1157996>
47. Seol, J.H. and Jo, I., Moore AL. Two-Dimensional Phonon Transport in Supported Graphene, *Science*, 2010, vol. 328(5975), pp. 213–216. <https://doi.org/10.1126/science.1184014>
48. Murmu, T. and Pradhan, S.C., Vibration Analysis of Nano-Single-Layered Graphene Sheets Embedded in Elastic Medium Based on Nonlocal Elasticity Theory, *J. Appl. Phys.*, 2009, vol. 105(6). <https://doi.org/10.1063/1.3091292>
49. Ansari, R. and Rouhi, S., Atomistic Finite Element Model for Axial Buckling of Single-Walled Carbon Nanotubes, *Phys. E: Low-Dimens. Syst. Nanostructures*, 2010, vol. 43(1), pp. 58–69. <https://doi.org/10.1016/j.physe.2010.06.023>
50. Arash, B., Wang, Q., and Liew, K.M., Wave Propagation in Graphene Sheets with Nonlocal Elastic Theory Via Finite Element Formulation, *Comput. Methods Appl. Mech. Eng.*, 2012, vol. 223, pp. 1–9. <https://doi.org/10.1016/j.cma.2012.02.002>
51. Arani, A.G. Haghparast, E., and Babaakbar Zarei, H., Nonlocal Vibration of Axially Moving Graphene Sheet Resting on Orthotropic Visco-Pasternak Foundation under Longitudinal Magnetic Field, *Phys. B. Condens.*, 2016, vol. 495, pp. 35–49. <https://doi.org/10.1016/j.physb.2016.04.039>
52. Xiao, W., Li, L., and Wang, M., Propagation of In-Plane Wave in Viscoelastic Monolayer Graphene Via Nonlocal Strain Gradient Theory, *Appl. Phys. A*, 2017, vol. 123(6), pp. 1–9. <https://doi.org/10.1007/s00339-017-1007-1>

**Publisher's Note.** Pleiades Publishing remains neutral with regard to jurisdictional claims in published maps and institutional affiliations.